Measurement of hyperfine structure and isotope shifts in Gd II

Dylan F. Del Papa, Christopher D.M. Rose, S. David Rosner, Richard A. Holt *

Department of Physics and Astronomy, University of Western Ontario, London, ON, Canada N6A 3K7

ABSTRACT

We have applied fast-ion-beam laser-fluorescence spectroscopy to measure the isotope shifts of 73 optical transitions in the wavelength range 421.5–455.8 nm and the hyperfine structures of 35 even parity and 33 odd parity levels in Gd II. Many of the isotope shifts and hyperfine structure measurements are the first for these transitions and levels. These atomic data can be used to correct for saturation and blending in the analysis of stellar spectra to determine chemical abundances. As a result, they have an important impact on studies of the history of nucleosynthesis in the Universe and on the use of photospheric abundance anomalies in Chemically Peculiar stars to infer indirect information about stellar interiors.

© 2017 Elsevier Ltd. All rights reserved.

1. Introduction

Laboratory measurements of atomic properties provide essential data for astrophysics, notably in the areas of: (a) studies of the history of nucleosynthesis in the Universe [1–3] by determining chemical abundances in very old ('extremely metal-poor') stars [4]; (b) indirect probing of the dynamics of stellar interiors by measuring surface (photospheric) chemical abundance anomalies in Chemically Peculiar stars [5] and by asteroseismology [6]; and (c) Solar and solar-metallicity stellar abundance studies [7–9].

Although much has been learned about the history of nucleosynthesis, many important questions remain, particularly with regard to the neutron-capture elements [2,3], *i.e.* elements with $Z > 30$ that cannot be formed by fusion because of the Coulomb barrier. Neutron capture occurs mainly through the slow 's-process' or the rapid 'r-process.' In the s-process, thought to take place in thermally pulsing Asymptotic Giant Branch stars, hundreds or thousands of years pass between successive neutron captures, allowing time for the nuclei to β decay, and thus the process follows the 'valley of β stability.' The r-process requires a far more intense neutron flux such as that in the environment of a supernova, and very rapidly builds up neutron-rich isotopes along a path far from the valley of β stability, eventually stabilizing by β decay. These two processes result in characteristically different chemical abundance patterns that can be used to probe the nucleosynthesis history. The r-process is of particular interest [10], as much remains to be determined, including even the sites at which it occurs, commonly thought to be the high-entropy (neutrino) wind of a Type II supernova [11–13]. Other suggestions are the merger of a neutron star with another neutron star or with a black hole [14–16].

Stellar interiors are quite difficult to study, as direct observation (in the visible portion of the spectrum) cannot penetrate deeper than the photosphere of a star. Nevertheless, determinations of surface abundance anomalies, combined with theoretical models [7], provide indirect information about the stellar interior. Although the bulk chemical abundances of a star are characteristic of the Interstellar Medium at the time the star was formed, outward diffusion of particular elements via the competition between radiation pressure, gravity, and convection can greatly affect the surface abundances, particularly in the Chemically Peculiar (CP) group of stars.

In order to infer chemical abundances from observed absorption lines in stellar spectra, astrophysicists need atomic data, first and foremost wavelengths and absorption oscillator strengths, but more subtly isotope shifts (IS) and hyperfine structure (hfs). Neither IS nor hfs can be resolved in stellar spectra; nevertheless, they play an important role in abundance determinations. As first pointed out by Abt [17], splitting a spectral line into several components de-saturates it, and an analysis that neglects this will derive erroneous chemical abundances. For example, Jomaron et al. [18] found that strong Mn II lines in HgMn stars gave inferred abundances that were wrong by 2–3 orders of magnitude, and they suggested that the discrepancy was due to hfs, for which no laboratory data were available at that time. We then carried out the first hfs measurements in Mn II [19] and solved the problem.

Gd is an r-process element that is located in the second neutron-capture abundance peak [3]. It has seven stable isotopes, some of whose properties are listed in Table 1. Of these, ^{160}Gd is made only by the r-process, ^{152}Gd and ^{154}Gd only by the s-process,

Table 1
Properties of the stable Gd isotopes. I, μ_I, and Q are the nuclear spin, magnetic dipole moment, and electric quadrupole moment, respectively.

Isotope	Mass (u)[a]	Abundance (%)[b]	I[c]	μ_I (nm)[c]	Q (b)[c]
^{152}Gd	151.9197910 (27)	0.20 (1)	0		
^{154}Gd	153.9208656 (27)	2.18 (3)	0		
^{155}Gd	154.9226220 (27)	14.80 (5)	3/2	−0.2572 (4)	1.30 (2)
^{156}Gd	155.9221227 (27)	20.47 (4)	0		
^{157}Gd	156.9239601 (27)	15.65 (3)	3/2	−0.3373 (6)	1.36 (2)
^{158}Gd	157.9241039 (27)	24.84 (12)	0		
^{160}Gd	159.9270541 (27)	21.86 (4)	0		

[a] Ref. [23].
[b] Ref. [24].
[c] Ref. [25].

and the others by a combination of both processes [3]. Altogether, 82% of the solar-system abundance of Gd is due to the r-process. Measurements of its abundance have played a role in studies of early neutron-capture nucleosynthesis [2,20], carbon-enhanced metal-poor stars [21], star formation in solar-metallicity stars [9], the Solar spectrum [7], and studies of ro-Ap stars [22].

The spectrum of Gd II has been studied by Albertson et al. [26], Russell [27], Blaise and van Kleef [28], Spector [29,30], and Blaise, van Kleef and Wyart [31]. Atomic lifetimes in Gd II have been measured by Zhang et al. [32], Xu et al. [33], Feng et al. [34], and Wang et al. [35]. Oscillator strengths have been obtained from lifetime measurements combined with branching-fraction measurements by Bergström et al. [36], Den Hartog et al. [37], and Wang et al. [38]. Surprisingly little attention has been devoted to the measurement of hfs in Gd II. To our knowledge, the only previous hfs measurements are those of Clieves and Steudel [39], using Fabry-Pérot spectroscopy on an enriched ^{157}Gd sample. They did not resolve the hfs, but by fitting components to their lineshapes, they obtained magnetic dipole and electric quadrupole hfs parameters for 18 levels. An early study by Suwa [40] provided some information about IS in two Gd II transitions. Measurements of IS by Brix and Lindenberger [41], Ahmad et al. [42,43], Kropp et al. [44], and Venugopalan et al. [45] have mostly concentrated in the UV region of the spectrum; however, Ref. [43] contains many visible transitions which can be compared with ours. In the present work, we have carried out an extensive series of high-resolution measurements of hfs and IS in a natural isotopic mixture of Gd II.

2. Experimental method

The experiment was carried out with fast-ion-beam laser spectroscopy (FIBLAS) [46]. This method offers many advantages. It is completely selective for mass-to-charge ratio, has high signal-to-noise ratios, yields very high spectral resolution as a result of kinematic compression [47], and spreads out the signals from the various isotopes because different masses acquire different velocities, and hence different Doppler shifts, from acceleration through the same potential drop. In our apparatus (see Fig. 1), Gd$^+$ ions are created within a Penning ion source we developed by modifying a commercial instrument to yield narrower beam-energy spreads [48]. Gd is introduced by sputtering from solid Gd cathodes into a Ne discharge.

The ions are extracted by a 10-kV potential difference between the cathode of the source and an extractor cone that forms part of the first element of an einzel lens (E1). The focused beam then passes through a Wien velocity filter, which serves as a mass spectrometer to remove the sizeable Ne$^+$ beam component ($\sim 1 \ \mu$A). This reduces space-charge spreading and greatly reduces the background light signal due to ion collisions with residual gas in the 5×10^{-6} Torr vacuum. (This elevated pressure is mainly due to Ne gas exiting the source; without this flow, the pressure is 5×10^{-7} Torr.) The mass resolution of the Wien filter is deliberately set to a low value to transmit all of the Gd isotopes with nearly equal efficiency, while still removing the Ne$^+$. The typically 200–300 nA Gd$^+$ beam is focused, steered, and then deflected through 5° to make it collinear with the laser beam. In a carefully designed 'Doppler tuning' region (DTR) that maintains a very uniform –478 V potential over a length of ~ 0.9 cm, the Doppler-shifted laser frequency comes into resonance with the ion's rest-frame optical transition frequency, inducing absorption followed by spontaneous emission, i.e., laser-induced fluorescence (LIF). An array of 80 optical fibers collects the LIF and transmits it outside the vacuum chamber to a bialkali photomultiplier (PMT) equipped with a UV bandpass filter (F) to block scattered laser light. Most of the LIF is in the UV because we excite transitions from metastable states and much of the strong spontaneous emission is to lower-lying states. Downstream from the Doppler tuning region, a further electrostatic deflection separates the ion beam from the laser beam again, steering it into a collector plate (FC) for monitoring the current.

The single-frequency CW laser beam in the Stilbene 420 wavelength range (420–460 nm) is produced by a ring dye laser (Coherent 699-21) pumped by the all-lines UV output of a high-power argon-ion laser (Coherent Sabre DBW-25/7). The typical
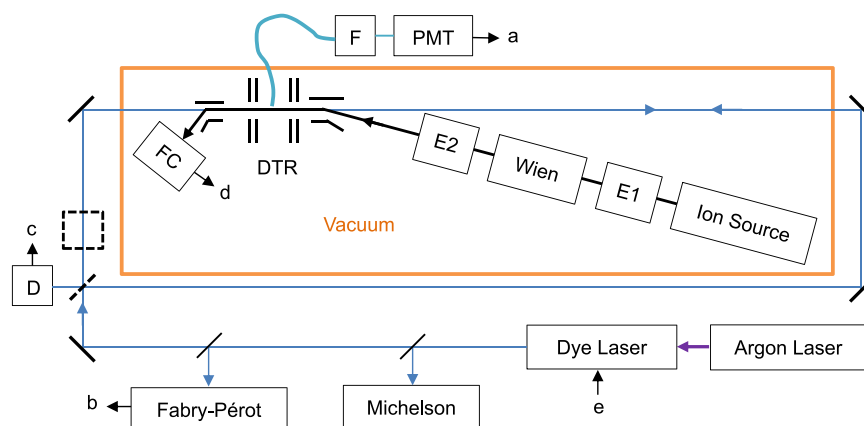
Fig. 1. Block diagram of the experimental apparatus. Wien: Wien velocity/mass filter; E1, E2: einzel focusing lenses; DTR: Doppler-tuning region; FC: Faraday collector for ion beam current; F: UV bandpass filter; PMT: photomultiplier tube; D: photodiode light detector; a, b, c, d: signals to data acquisition system (a, c, and d are conditioned by electrometers); e: scanning staircase ramp from data acquisition system. Dashed mirror is inserted for parallel geometry; dashed rectangle shows position of light detector D in this case. Optical fiber bundle from DTR to F contains 80 fibers. Additional electrostatic deflection plates are not shown for simplicity.